Available online at www.sciencedirect.com
SCIENCE DIRECT®
Materials Chemistry and Physics 87 (2004) 275–284
MATERIALS CHEMISTRY AND PHYSICS
www.elsevier.com/locate/matchemphys

A TEA-starch combustion method for the synthesis of fine-particulate $LiMn_2O_4$

G. Ting-Kuo Fey*, Yung-Da Cho, T. Prem Kumar[1]

Department of Chemical and Materials Engineering, National Central University, Chung-Li 32054, Taiwan, ROC

Received 29 December 2003; received in revised form 8 April 2004; accepted 5 May 2004

Abstract

Solution combustion synthesis of fine-particulate $LiMn_2O_4$ was carried out with triethanolamine (TEA) and starch as fuels. TEA:starch ratio, calcination temperature and duration of calcination were varied in order to obtain $LiMn_2O_4$ with optimal electrochemical properties. Increasing the starch content in the precursor was found to be detrimental to product characteristics. Although the product prepared with a TEA:starch ratio of 1:1 by a 10 h calcination at 800 °C showed the highest first-cycle capacity (127 mAh g^{-1}), the cyclability was the highest for the product synthesized by a 500 °C 10 h calcination of a 1:1 TEA:starch precursor. The latter sample sustained 75 cycles at a 0.1*C* rate between 3.0 and 4.3 V before reaching 80% capacity retention. The electrochemical properties of the products are explained in terms of their structural and morphological properties as well as the local reaction environments during the formation processes.

Keywords: $LiMn_2O_4$; Combustion synthesis; Cathode; Intercalation; Lithium-ion battery

1. Introduction

The stoichiometric spinel $LiMn_2O_4$ phase represents a prospective lithium-intercalating cathode material for lithium-ion batteries. $LiMn_2O_4$ offers benefits such as low price, natural abundance and environmental friendliness of manganese precursor materials, thermal stability of the spinel, and the battery industry's familiarity with manganese oxide chemistry. Reversible electrochemical extraction of lithium ions from $LiMn_2O_4$ proceeds at about 4 V versus Li^+/Li. Although the charge–discharge processes in the 4 V region are accompanied by a 7.6% volume change in the unit cell, the change is so gradual and isotropic that the cubic symmetry of the material is usually maintained [1,2]. However, prolonged cycling, especially at elevated temperatures, results in a capacity fade [3–5]. In addition to cycle life, high-rate and low-temperature performance must also be addressed before the cathode material can be considered for challenging requirements such as for vehicular traction applications. Therefore, much research is directed towards synthesizing lithium–manganese spinel oxides with characteristics that can meet these requirements.

The electrochemical behavior of $LiMn_2O_4$ is strongly influenced by the method of preparation, as well as the precursors and heat treatment protocols. Synthesis parameters determine the crystallinity, phase purity, particle morphology, grain size, surface area, and cation distribution in the spinel structure, all of which can impact on the electrochemical performance of the spinel [6,7]. Such oxides have conventionally been synthesized by diffusion-limited solid-state fusion methods with their associated repeated grinding and high temperature operations. To obviate the need for such cumbersome, and often energy-intensive procedures, several innovative low-temperature synthesis procedures have been adopted for the preparation and processing of solid oxide materials [8,9]. One such approach is combustion synthesis, which involves highly exothermic redox chemical species in flaming (gas-phase), smouldering (heterogeneous), or explosive reactions [9–13].

Since the serendipitous synthesis of α-alumina by rapid heating of aluminum nitrate-urea solutions [14], much interest has been evinced in solution-based combustion synthesis of oxidic materials. This method provides several advantages: simple and economical preparation, easy control of homogeneity and stoichiometry, easy incorporation of dopants/substituents, production of fine-particulate, high

* Corresponding author. Tel.: +886 3 425 7325/886 3 422 7151extn.4206; fax: +886 3 425 7325.
E-mail address: gfey@cc.ncu.edu.tw (G.T.-K. Fey).
[1] On deputation from the Central Electrochemical Research Institute, Karaikudi 630006, TN, India.

0254-0584/$ – see front matter © 2004 Elsevier B.V. All rights reserved.
doi:10.1016/j.matchemphys.2004.05.009

surface area materials by virtue of the accompanying gas evolution, and versatility in terms of the variety of fuels that can be used for the synthesis. In this paper, we present our results on the synthesis, characterization and electrochemical behavior of $LiMn_2O_4$ synthesized with triethanolamine (TEA) and starch as fuels, and nitrates of manganese and lithium as the oxidants. The synthesis involves the molecular dispersion of a precursor of the reagents in a polymeric matrix of TEA and starch, followed by deflagration to the oxidic product in a carbonaceous substrate. Subsequent calcination yields finely divided $LiMn_2O_4$.

2. Experimental

The synthesis of $LiMn_2O_4$ was carried out at different TEA:starch mole ratios (1:1, 1:2, 1:4, 1:8, and 1:16). All mixtures had a TEA:total cations mole ratio of 1:1. Typically, stoichiometric amounts of $LiNO_3$ and $Mn(NO_3)_2{\cdot}4H_2O$ were dissolved in a minimum volume of double distilled water. The required amount of TEA was added and stirred until a clear solution was obtained. To this mixture, an appropriate amount of starch was added. The pH of the mixture, which was between 6 and 7, was adjusted to 3.5 by adding nitric acid. This mixture was then heated at 180 °C on a hot plate inside a fume hood. As the heating progressed, the volume of the mixture gradually increased, resulting in a brown jelly mass. With continued heating, the jelly mass charred and slowly deflagrated with the evolution of brownish gases. The resultant black carbonaceous fluffy mass was used as the precursor for preparing the $LiMn_2O_4$ powders, which were obtained by calcination at different temperatures for varying durations.

Structural properties of the synthesized materials were studied by the X-ray diffraction method (Siemens D5000). Diffraction patterns were recorded with nickel-filtered Cu Kα radiation between scattering angles of 5° and 80° in increments of 0.05°. The surface morphology of the particles was studied by scanning electron microscopy (Hitachi S-4700I) and by field-emission scanning electron microscopy (Hitachi S800). BET surface area measurements were done by the nitrogen adsorption–desorption method (Micromeritics ASAP 2010).

Charge–discharge studies were carried out with coin cells assembled in standard 2032 stainless steel cell hardware. Lithium metal was used as the anode and a 1 M solution of $LiPF_6$ in EC:DEC (1:1 v/v) was used as the electrolyte. The cathode was prepared by blade-coating a slurry of 85 wt.% active material with 10 wt.% conductive carbon black and 5 wt.% PVdF binder in NMP on an aluminum foil, drying overnight at 120 °C in an oven, roller-pressing the dried coated foil, and punching out circular discs. Cell assembly was done in an argon-filled glove box (VAC, MO 40-1), which contained less than 2 ppm oxygen and moisture. The cells were cycled between 3.0 and 4.3 V at a 0.1*C* rate (Maccor 4000 multi-channel battery tester).

3. Results and discussion

3.1. X-ray diffraction studies

The X-ray diffractograms of $LiMn_2O_4$ synthesized with different TEA:starch ratios under a 10 h calcination at 800 °C are shown in Fig. 1. All the diffractograms show patterns corresponding to the cubic spinel structure in *Fd3m* space group. It can be seen that as the starch content was increased, in addition to a slight broadening of the peaks, some extraneous peaks began to appear in the diffractograms. This suggests that at higher starch levels, the heat generated by the combustion process was muffled, thereby rendering the crystallization of the spinel oxide less efficient. Table 1 presents the lattice and crystallographic parameters for the above $LiMn_2O_4$ products. It can be seen that there was a general increase in the value of the lattice parameter *a* as the starch content was increased. While the Mn^{3+} and Mn^{4+} ions occupy only the 16*d* octahedral sites in the spinel [15], the Li^+ ions can occupy both 8*a* tetrahedral and 16*d* octahedral sites [15–17]. Thus, in the spinel structure, the manganese ions in the spinel can be easily replaced by lithium ions [16,18]. The peak intensities of closely located reflections can be used as an index of cation disorder in $LiMn_2O_4$. Table 1 shows that the intensity ratio I_{400}/I_{311} decreased up to the 1:8 ratio, and then increased as the amount of starch was increased. On the other hand, the value of the intensity ratio I_{220}/I_{311} increased as the proportion of starch was increased. It appears that a large amount of starch is not conducive to good crystalline order. The values of the lattice parameter *a* were less than the 8.244 Å reported in literature [19].

Fig. 2 presents the X-ray diffractograms of $LiMn_2O_4$ synthesized with a TEA:starch ratio of 1:1 at different temperatures. The duration of calcination was 10 h. Here again, all the diffraction peaks were indexable in the *Fd3m* cubic symmetry. However, the diffractograms of the materials obtained by calcination at 500 and 600 °C show broad profiles, indicating the reduced crystallinity of these products. As the calcination temperature was increased, the reflections were found to get sharper, indicating the increasing crystallinity of the products. In the *Fd3m* cubic spinel structure, the (4 0 0) reflection is very sensitive to the calcination temperature, evidenced by the increasing sharpness of the (4 0 0) peak with increasing calcination temperature. As can be seen from Table 1, the value of the lattice parameter *a*, generally increased as the temperature was raised. It is generally believed that the lattice parameter in the cubic spinel structure depends on the manganese valence state. In low-temperature products, a significant fraction of manganese ions are present in the Mn^{4+} state because of the greater stability of Mn^{4+} ions at low temperatures [20]. Therefore, the smaller Mn^{4+} ions (Mn^{4+}: 0.60 Å; Mn^{3+}: 0.68 Å [21]) leads to diminished values of *a*. With the replacement of a part of the Mn^{4+} ions with Mn^{3+} ions at the higher temperatures, the cubic lattice parameter also increases.

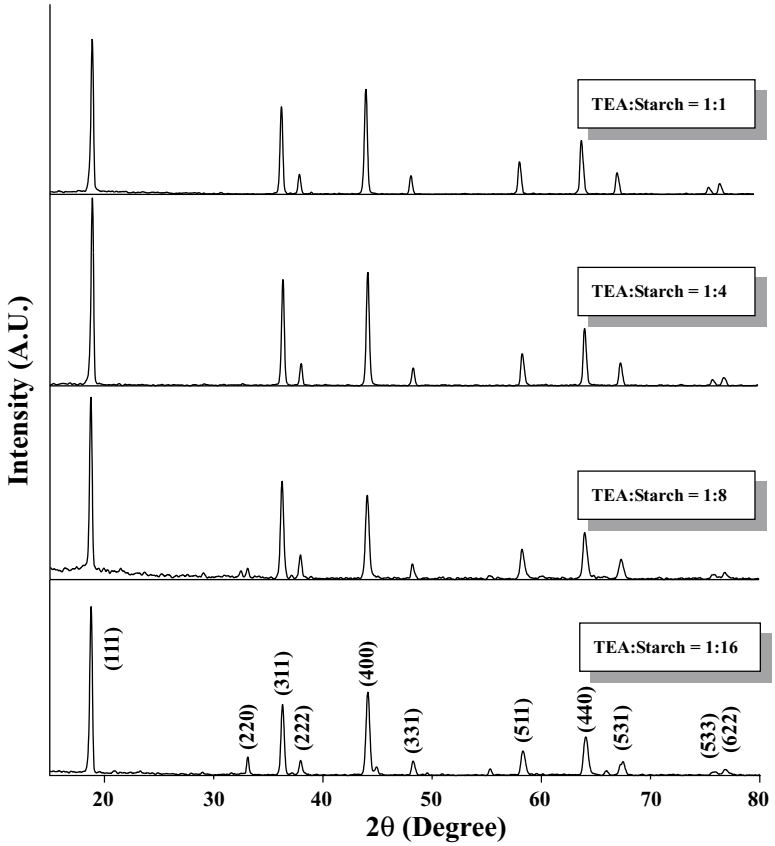

Fig. 1. X-ray diffractograms of $LiMn_2O_4$ synthesized with different TEA:starch ratios. Calcination: 800 °C, 10 h.

The X-ray diffractograms of $LiMn_2O_4$ synthesized with a TEA:starch ratio of 1:1 by calcination at 500 °C for different durations showed that the diffractograms tended to become sharper as the calcination period was increased, indicating that the crystallinity of the products improved with the duration of calcination. Lattice parameters of the different products are presented in Table 1.

3.2. Surface area and morphology

The scanning electron micrographs of the products obtained at the various TEA:starch ratios (10 h calcination at 800 °C) are shown in Fig. 3. Fine particulates, of undefined morphology and particle size typically less than 1 μm, can be seen at a 1:1 TEA:starch ratio. The particles were found to grow as the starch content was increased, finally turning into nearly well-sintered particles of 2–10 μm at a TEA:starch ratio of 1:16. The BET surface areas of the products are summarized in Table 2. As can be seen from the table, the sample synthesized at a TEA:starch ratio of 1:1 had the largest surface area (4.56 $m^2\ g^{-1}$). In the present study, decreasing the TEA to starch ratio to 1:4, 1:8 and 1:16 resulted in a decreased surface area (Table 2). TEA helps in the dispersion of the cations in the carbonaceous matrix, which is formed

Table 1
Crystallographic parameters for $LiMn_2O_4$ products

TEA:starch	Calcination		Lattice parameter '*a*' (Å)	I_{400}/I_{311}	I_{220}/I_{311}	Unit cell volume $(Å)^3$
	Temperature (°C)	Duration (h)				
1:16	800	10	8.204	1.17	0.26	552.1
1:8	800	10	8.214	0.86	0.09	554.3
1:4	800	10	8.193	1.07	0.00	550.0
1:1	800	10	8.197	1.20	0.00	550.7
1:1	700	10	8.241	0.97	0.00	559.7
1:1	600	10	8.236	1.00	0.00	558.7
1:1	500	10	8.233	1.00	0.00	558.1
1:1	500	20	8.232	0.94	0.00	557.8
1:1	500	5	8.225	1.09	0.00	556.4

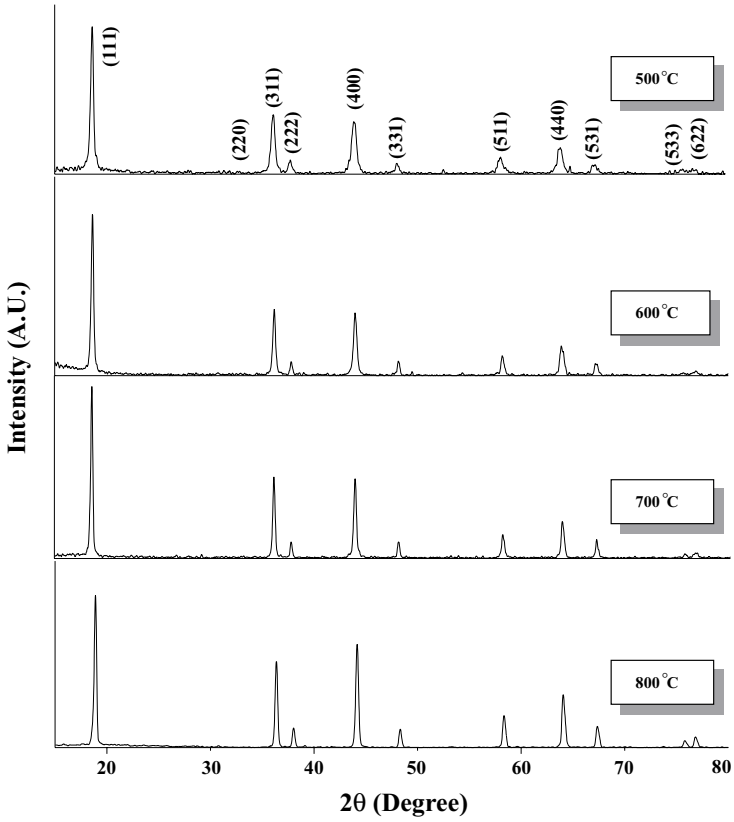

Fig. 2. X-ray diffractograms of $LiMn_2O_4$ synthesized with a TEA:starch ratio of 1:1 by a 10 h calcination at different temperatures.

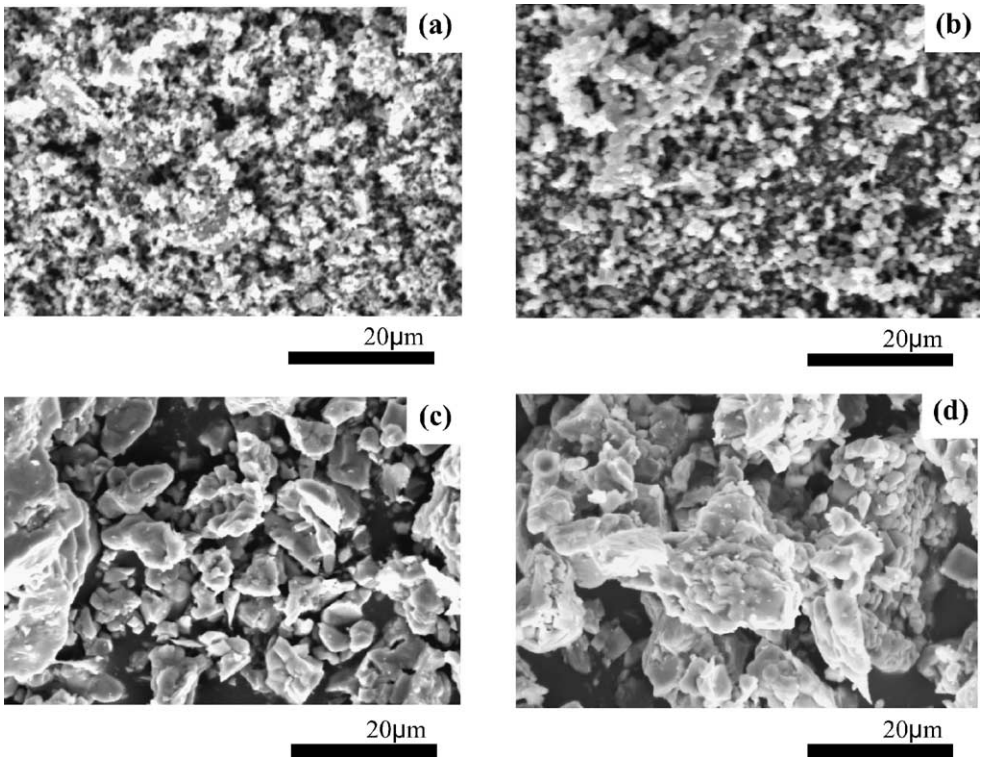

Fig. 3. Scanning electron micrographs of $LiMn_2O_4$ obtained at various TEA:starch ratios. Calcination: 800 °C, 10 h. TEA:starch ratios: (a) 1:1; (b) 1:4; (c) 1:8; (d) 1:16.

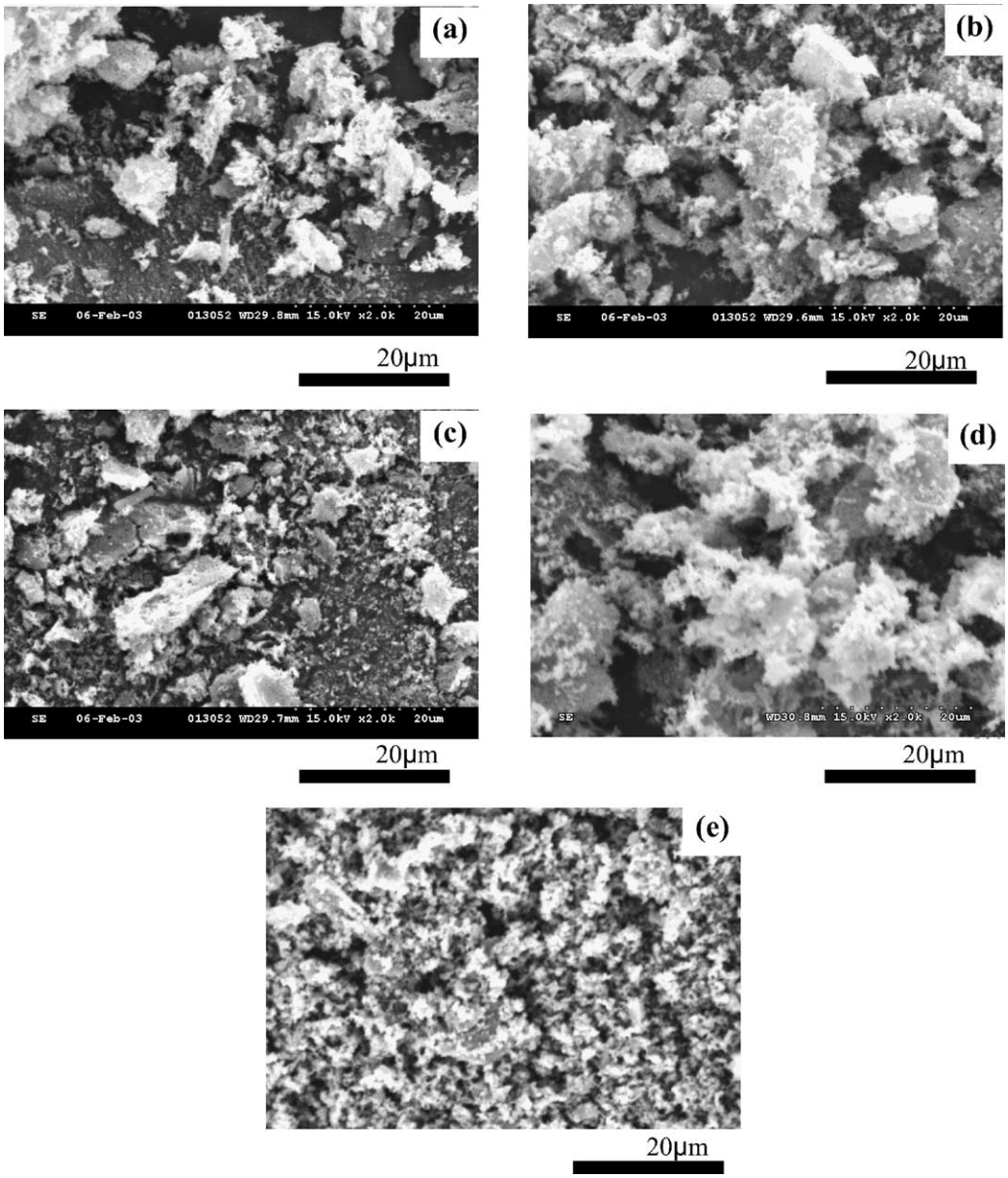

Fig. 4. Effect of temperature on the morphology of $LiMn_2O_4$ obtained by a 10 h calcination of a 1:1 (TEA:starch) precursor. (a) 400 °C; (b) 500 °C; (c) 600 °C; (d) 700 °C; (e) 800 °C.

upon its carbonization. Decreasing the TEA amount would lead to less chelation of the cations and lower levels of cation distribution. From another perspective, an increase in the amount of starch would lead to a swift rise in temperature in a narrow timeframe due to the combustion of starch. Thus, increased amounts of starch should lead to a sintering of the particles. The decrease in surface area with an increase in the amount of starch corroborates this reasoning.

Table 2
BET surface areas for select $LiMn_2O_4$ samples

TEA:starch (800 °C, 10 h)	BET surface area ($m^2\,g^{-1}$)
1:1	4.56
1:4	1.49
1:8	0.08
1:16	0.05

Janbey et al. [22], who synthesized nanocrystalline α-Al_2O_3 with sucrose as a fuel, found that sucrose played an important role in the formation of unagglomerated alumina. According to these authors [22], sucrose forms a carbonaceous matrix upon decomposition, which acts as a substrate for the homogeneous distribution of the metal oxide phase. Upon calcination in air, the carbonaceous substrate is oxidized to carbon dioxide, leaving behind a finely divided oxide phase. In our case, we had two complexing species: triethanolamine, with its three hydroxyl groups and the nitrogen atom, and the polyhydroxy starch.

The nitric acid added to the mixture converts the starch into a polyhydroxy acid [23]. These polyhydroxy acids, in addition to coordinating with the cations, cross-link with triethanolamine. Similar polymer branching has been observed with poly-(vinyl alcohol) [24]. Adding these chelating agents to a molecularly mixed solution of lithium and manganese ions would result in an immediate and strong bonding of the metal ions with the coordinating centers in the organic moieties to form micelles in which the cations are trapped in an organic environment. The micelle formation hampers selective precipitation of the metal ions during evaporation of the water from the solution. After prolonged heating, the viscous polymeric mass gets partially carbonized, providing a substrate in which the metal ions find themselves embedded. Eventually, the metal nitrates oxidize the polyhydroxy acid-triethanolamine polymer substrate, which acts as an internal fuel, yielding the desired product. The accompanying gas evolution helps break down large agglomerated particles.

From the electron micrographs (Fig. 3), it can be seen that an increase in the starch content in the starting mixtures led to more compact particles. According to Pati et al. [25], who used TEA as a complexing agent for the synthesis of Al_2O_3, TEA not only ensures a homogeneous distribution of metal ions, but also provides a mesoporous carbonaceous matrix upon decomposition, in which nascent atomic clusters of the metal oxide get embedded. Therefore, the higher the amount of TEA, the larger will be the surface area. Moreover, according to Pati et al. [25], polyhydroxy organic compounds also yield similar mesoporous carbon structures, but do so only in the absence of metal ions. The lower particle size of the materials synthesized with a TEA:starch ratio of 1:1 and 1:4 may be associated with the extensive distribution of mesoporous carbonaceous matrix which provided a larger number of well-separated nucleation sites for the oxide to form. This resulted in particles with lower size distribution. At the other extreme, at the lowest TEA:starch ratio (1:16), where distribution of metal ions in a uniform mesophase matrix is not favored, particles with more definitive morphologies and larger sizes resulted. Hence, the formation of the carbonaceous matrix and the Li–Mn-oxide phase has an optimal ratio of TEA and starch.

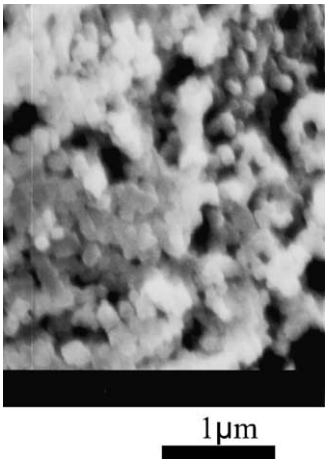

Fig. 5. An FE-SEM image of $LiMn_2O_4$ obtained at 700 °C.

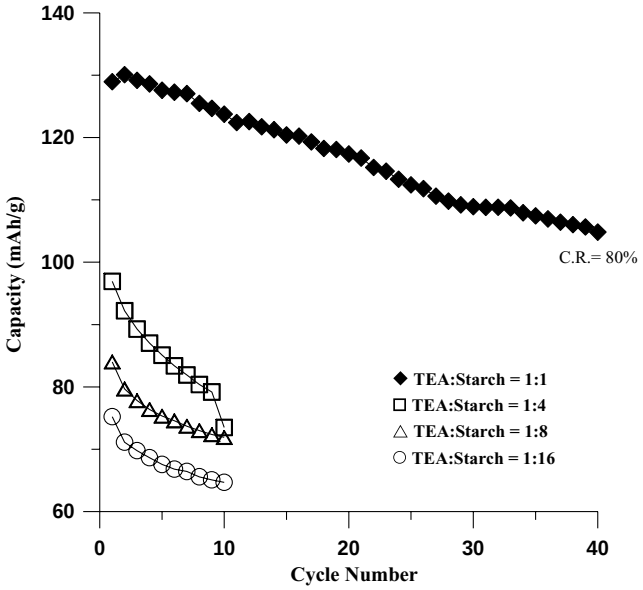

Fig. 6. Galvanostatic cycling performance of $LiMn_2O_4$ prepared with different TEA:starch ratios. Calcination: 800 °C, 10 h.

The effect of temperature on the morphology of the products obtained by a 10 h calcination of a 1:1 (TEA:starch) precursor is illustrated in Fig. 4. All the products appear to be agglomerates of fine particulates, with no well-defined morphology. An FE-SEM image of the product obtained at 700 °C is shown in Fig. 5. Nanocrystallites that constitute the agglomerates can be noticed. The complexation of the cations by TEA and their extensive distribution in

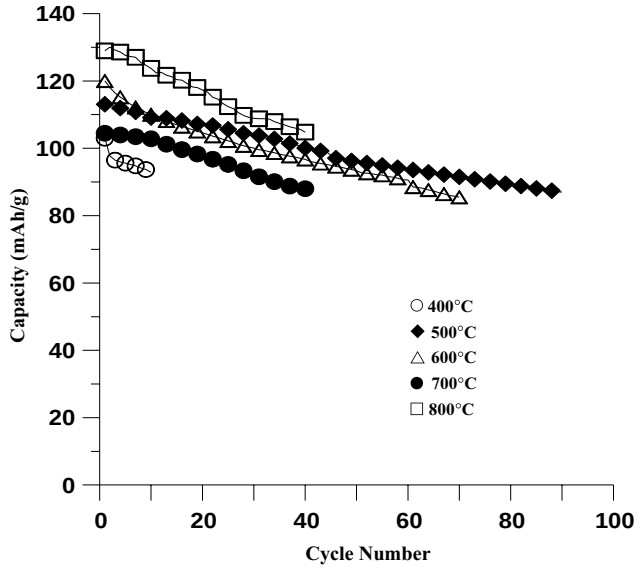

Fig. 7. Effect of 10 h calcination at different temperatures on the charge–discharge behavior of $LiMn_2O_4$ obtained at a 1:1 TEA:starch ratio.

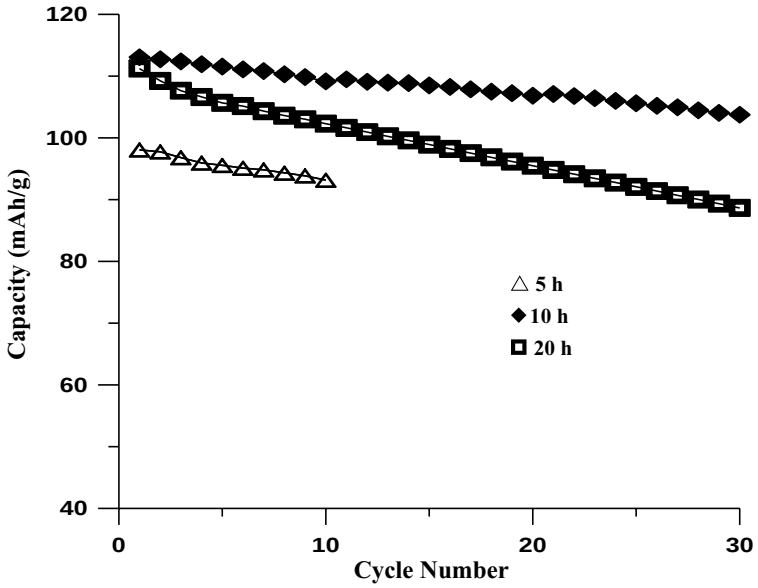

Fig. 8. Effect of duration of calcination on the cycling behavior of $LiMn_2O_4$ obtained at 500 °C from a 1:1 TEA:starch precursor.

the carbonaceous matrix ensure the production of such nanostructured products.

3.3. Charge–discharge studies

The galvanostatic cycling performance of the materials prepared with different TEA:starch ratios (800 °C, 10 h) is depicted in Fig. 6. For the material prepared with a TEA:starch ratio of 1:1, the discharge capacity was 127 mAh g^{-1} in the first cycle. The first-cycle capacity decreased as the starch amount was increased: they were 97, 84 and 75 mAh g^{-1} for TEA:starch ratios of 1:4, 1:8 and 1:16, respectively. We have already noted that the surface area of the products decreased with an increase in the starch content (Table 2). Thus, the capacities of the products were commensurate with the surface area: the larger the surface area, the larger the capacity. It is well known that the particle size and morphology of cathode materials have a definite effect on the electrochemical properties [27–30]. Small cathode active particles provide small diffusion pathways, resulting in an improvement in the lithium-ion intercalation kinetics [31].

Fig. 6 shows that the 1:1 (TEA:starch) sample could sustain 43 charge–discharge cycles before reaching an 80% cut-off value in capacity retention. However, the products obtained at the other TEA:starch ratios gave only about 10 cycles before reaching the 80% charge retention cut-off. Thus, it appears that the large surface area and small particle sizes promoted a definite improvement in the intercalation kinetics. The improved kinetics also allowed for longer cyclability due to the fact that the structural distortions at the surface of the small particles were minimal [31]. At the smaller surface areas, the active area available for electron transfer is limited. It is also possible that when excess starch

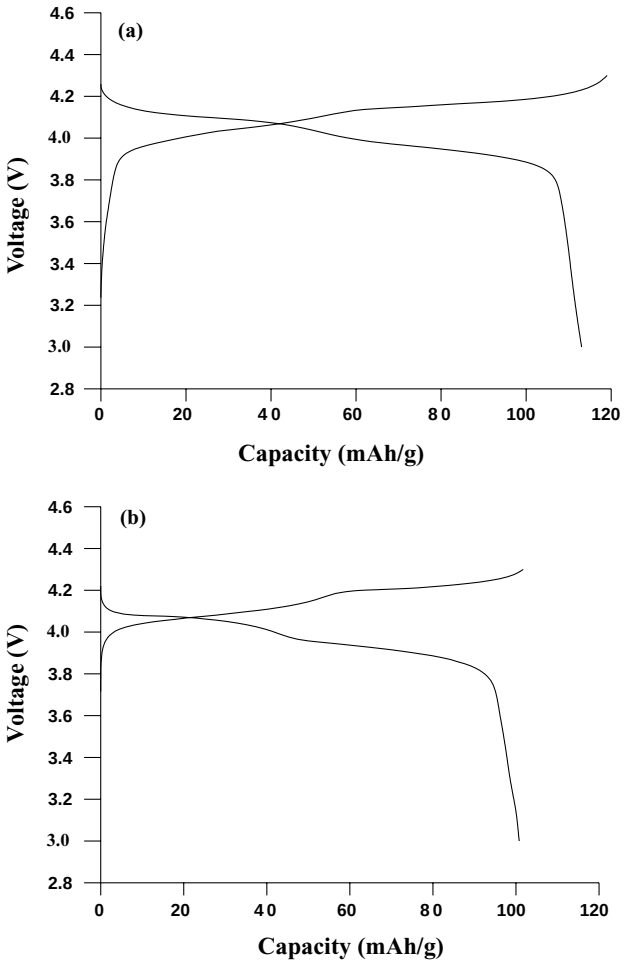

Fig. 9. Charge–discharge profiles of $LiMn_2O_4$ calcined at (a) 500 °C; (b) 800 °C. Duration of calcination: 10 h.

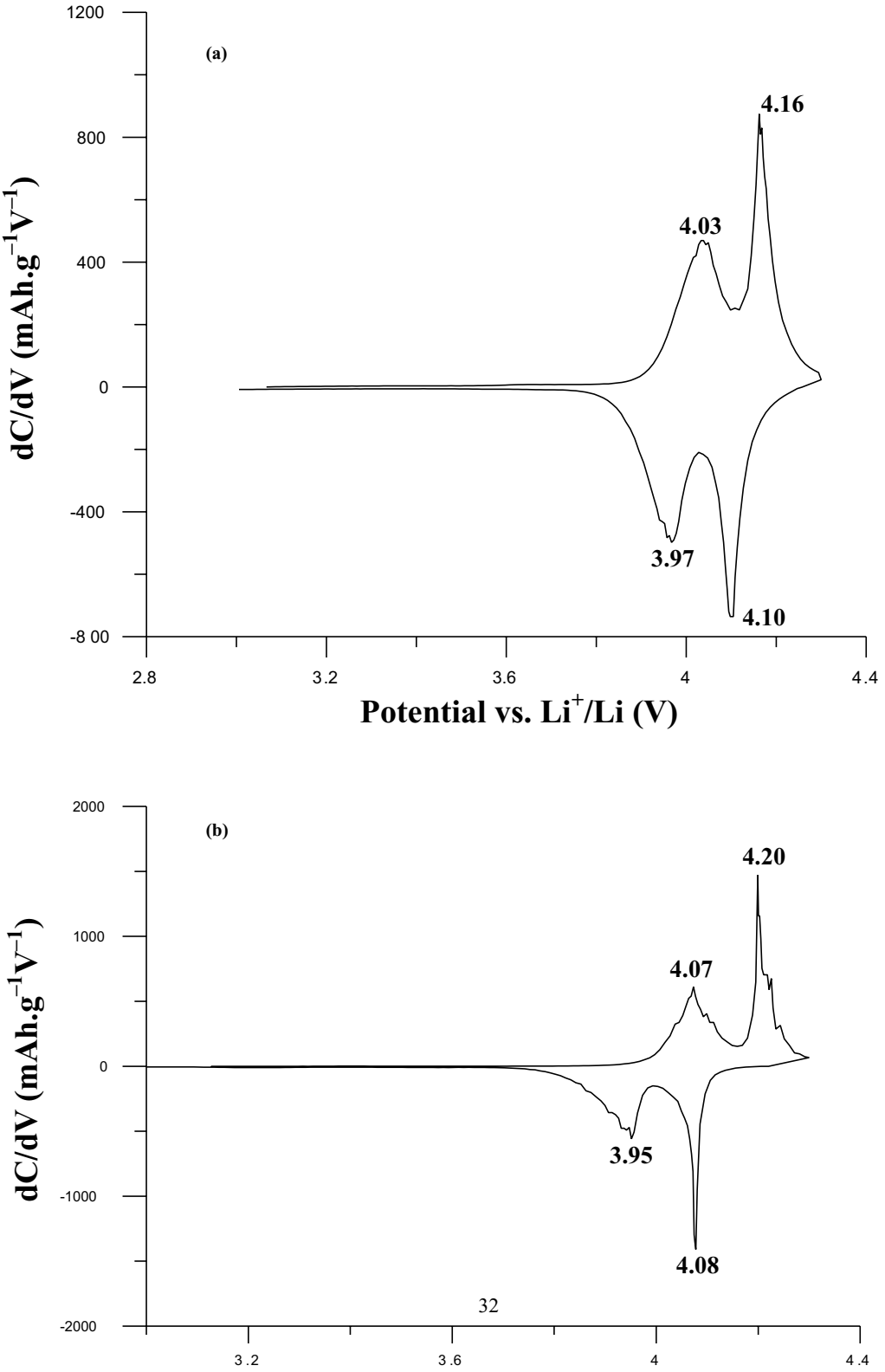

Fig. 10. Differential capacity curves of $LiMn_2O_4$ obtained by calcination at (a) 500 °C; (b) 800 °C. Duration of calcination: 10 h.

is present in the precursor mixtures, the gases released during combustion might reduce the local oxygen partial pressure, which can have a deleterious effect on the electrochemical properties of the system, as observed in the case of several layered transition metal oxides [32].

Having determined the optimal TEA:starch ratio to be 1:1, the effect of calcination temperature was studied. It must be mentioned here that a lower amount of starch (TEA:starch ratio 1:0.5) was also tried; however, the performance of the product was poor. Fig. 7 shows the effect of 10 h calcination at different temperatures on the charge–discharge behavior of the products obtained with a 1:1 TEA:starch ratio. The highest first-cycle capacity of 120 mAh g^{-1} was obtained for the product of the 600 °C calcination, while the capacities were lower for the materials calcined at temperatures lower and higher than 600 °C. On the other hand, the cyclability was the highest for the 500 °C product, whose first-cycle capacity was 113 mAh g^{-1}. This material sustained 75 cycles before reaching 80% capacity retention, while the 600 °C product could sustain only 41 cycles. The effect of duration of calcination on the cycling behavior was also investigated. For this, the product from the 1:1 TEA:starch precursor was calcined at 500 °C for 5, 10 and 20 h. The results are shown in Fig. 8. The figure shows that the first-cycle capacities for the 10 h and 20 h calcined samples (113 and 111 mAh g^{-1}, respectively) were higher than the capacity for the 5 h calcined sample (93 mAh g^{-1}). However, while the 10 h sample gave 75 cycles before reaching the 80% cut-off value in capacity retention, the 20 h sample sustained only 30 cycles. The inferior performance of the 5 h calcined material reflects the poor phase characteristics of the products, as revealed by the X-ray diffraction patterns. It is suggested that the loss of lithium on extended heating led to the poor cyclability of the 20 h calcined sample.

Fig. 9 shows the first-cycle charge–discharge profiles of the materials prepared by a 10 h calcination at 500 and 800 °C. A less obvious two-step charge–discharge profile was expected for the product of the lower temperature calcination because the two-step profile is a characteristic feature of crystalline $LiMn_2O_4$ spinels [26]. According to Ohzuku et al. [33] in the compositional range $0.27 \leq x \leq 0.60$ in $Li_xMn_2O_4$, two cubic phases ($a = 8.142$ and 8.045 Å) co-exist, giving rise to the plateaus at 3.94 and 4.11 V, respectively, and that the charge–discharge processes occur via a homogeneous phase between x values of 0.6 and 1.0. This is nearly consistent with the fractions of the capacities that each of these pseudo-plateaus account for. Liu et al. [19] suggest that each of these plateaus should deliver half of the total capacity, in accordance with the assumption that two cubic systems co-exist during the reversible lithium intercalation processes, viz. $LiMn_2O_4$–$Li_{0.5}Mn_2O_4$ and $Li_{0.5}Mn_2O_4$–λ-MnO_2. Because no difference could be discerned from the charge–discharge profiles of the products derived at 500 and 800 °C (Fig. 9), the first-cycle differential capacity curves of the two materials were plotted. Fig. 10 shows that both the materials yielded well-separated double peaks on the charging sweep as well as on the discharging sweep. However, the 800 °C-calcined material had sharper peaks compared to the 500 °C-calcined sample, suggesting the greater crystallinity of the former. The occurrence of the two peaks is attributed to the difference in the energies between lithium intercalation for values of x below and above 0.5 in $Li_xMn_2O_4$ [33–36]. It is believed that this energy difference arises because of a lithium ion ordering that must precede the greater occupation of the 8*a* tetrahedral sites [33–36]. The lower intensities of the double peaks obtained with the 500 °C-calcined material means a poor ordering of the 8*a* tetrahedral and 16*d* sites. In other words, in the low-temperature product, the charge–discharge processes occur by the diffusion of lithium ions in a less ordered lattice of $LiMn_2O_4$. Tsumura et al. [27] obtained low capacities from $LiMn_2O_4$ derived from tartaric acid at low temperatures. The poor capacity of these materials was attributed to the poor crystallinity, low lattice parameter and increase in lattice strain [27]. It is significant to note here that the lower amount of Mn^{3+} ions in the products synthesized at the lower temperatures not only led to a lower lattice parameter, as discussed previously, but also to reduced capacity, the Mn^{3+} being the capacity-yielding species in the 4 V region. Increasing the calcination temperature resulted in increased number of Mn^{3+} ions, as evidenced by the increase in the lattice parameters as well as the increase in capacity.

4. Conclusions

Fine-particulate $LiMn_2O_4$ was synthesized via a novel chemical route by using triethanolamine and starch as chelating internal fuels. Various TEA:starch ratios were studied in order to obtain $LiMn_2O_4$ with optimal electrochemical properties. Increasing the starch content in the precursor was found to be detrimental to product characteristics. The product prepared with a TEA:starch ratio of 1:1 by a 10 h calcination at 800 °C showed the largest surface area of 4.56 m^2 g^{-1}, and the highest first-cycle capacity of 127 mAh g^{-1}. However, the best cycling performance was obtained with a product synthesized by a 500 °C 10 h calcination of a 1:1 TEA:starch precursor. The sample sustained 75 cycles at a 0.1*C* rate between 3.0 and 4.3 V before reaching 80% capacity retention. The formation of the products and their electrochemical properties were explained in terms of the local reaction environments in the precursor mixtures.

Acknowledgements

Financial support by the National Science Council of the Republic of China under grant NSC-91/2811/E/008/002 is gratefully acknowledged. TPK thanks the National Science Council for the award of a post-doctoral fellowship.

References

[1] W.I.F. David, M.M. Thackeray, L.A. Picciotto, J.B. Goodenough, J. Solid State Chem. 67 (1987) 316.
[2] Y.K. Sun, Electrochem. Commun. 2 (2000) 6.
[3] Y. Xia, Y. Zhou, M. Yoshio, J. Electrochem. Soc. 144 (1997) 2593.
[4] R.J. Gummow, A. de Kock, M.M. Thackeray, Solid State Ionics 69 (1994) 59.
[5] G.G. Amatucci, C.N. Schmutz, A. Blyr, C. Sigala, A.S. Gozdz, D. Larcher, J.M. Tarascon, J. Power Sour. 69 (1997) 11.
[6] J.M. Tarascon, W.R. McKinnon, F. Coowar, T.N. Bowmer, G.G. Amatucci, D. Guyomard, J. Electrochem. Soc. 141 (1994) 1421.
[7] Y. Gao, J.R. Dahn, J. Electrochem. Soc. 143 (1996) 100.
[8] C.N.R. Rao, Chemical Approaches to the Synthesis of Inorganic Materials, Wiley-Eastern, New Delhi, 1994, p. 28.
[9] A.G. Merzhanov, in: C.N.R. Rao (Ed.), Chemistry of Advanced Materials: A Chemistry for the 21st Century, Blackwell, London, 1993, p. 19.
[10] A.G. Merzhanov, Int. J. Self-Propag. High-Temp. Synth. 2 (1993) 113.
[11] J.J. Moore, H.J. Feng, Prog. Mater. Sci. 39 (1995) 275.
[12] K.C. Patil, S.T. Aruna, S. Ekambaram, Curr. Opin. Solid State Mater. Sci. 2 (1997) 158.
[13] T. Mimani, J. Alloys Compd. 315 (2001) 123.
[14] J.J. Kingsley, K.C. Patil, Mater. Lett. 6 (1998) 427.
[15] T. Ohzuku, K. Ariyoshi, S. Takeda, Y. Sakai, Electrochim. Acta 46 (2001) 2327.
[16] T. Ozhuku, S. Kitano, M. Iwanaga, H. Matsuno, A. Ueda, J. Power Sour. 68 (1997) 646.
[17] T. Ohzuku, A. Ueda, Solid State Ionics 69 (1994) 201.
[18] M.M. Thackeray, J. Electrochem. Soc. 144 (1997) L100.
[19] W. Liu, G.C. Farrington, F. Chaput, B. Dunn, J. Electrochem. Soc. 143 (1996) 879.
[20] C. Masquelier, M. Tabuchi, K. Ado, R. Kanno, Y. Kobayashi, Y. Maki, O. Nakamura, J.B. Goodenough, J. Solid State Chem. 123 (1996) 255.
[21] W. Borchardt-Ott, Crystallography, Springer, New York, 1993.
[22] A. Janbey, R.K. Pati, S. Tahir, P. Pramanik, J. Eur. Ceram. Soc. 21 (2001) 2285.
[23] J.C. Ray, P. Pramanik, S. Ram, Mater. Lett. 48 (2001) 281.
[24] P. Pramanik, Bull. Mater. Sci. 18 (1995) 819.
[25] R.K. Pati, J.C. Ray, P. Pramanik, J. Am. Ceram. Soc. 84 (2001) 2849.
[26] J.M. Tarascon, E. Wang, F.K. Shokoohi, W.R. McKinnon, S. Colson, J. Electrochem. Soc. 138 (1991) 2859.
[27] T. Tsumura, A.S. Shimizu, M. Inagaki, Solid State Ionics 90 (1996) 197.
[28] Z. Jiang, K.M. Abraham, J. Electrochem. Soc. 143 (1996) 1591.
[29] J. Kim, A. Manthiram, Nature 390 (1997) 265.
[30] S.H. Kang, J.B. Goodenough, L.K. Rabenberg, Electrochem. Solid-State Lett. 4 (2001) A49.
[31] P. Lucas, C.A. Angell, J. Electrochem. Soc. 147 (2000) 4459.
[32] Y.K. Sun, I.H. Oh, J. Mater. Sci. Lett. 16 (1997) 30.
[33] T. Ohzuku, M. Kitagawa, T. Hirai, J. Electrochem. Soc. 137 (1990) 769.
[34] Y.S. Han, H.G. Kim, J. Power Sour. 88 (2000) 161.
[35] M.H. Rossouw, A. de Kock, L.A. de Picciotto, M.M. Thackeray, W.I.F. David, R.M. Ibberson, Mater. Res. Bull. 25 (1990) 173.
[36] J.M. Tarascon, F. Coowar, G.G. Amatucci, F.K. Shokoohi, D. Guyomard, J. Power Sour. 54 (1995) 103.